The Infrared Spectrum of the Matrix-Isolated Phenyl Radical

Anders V. Friderichsen,[§] Juliusz G. Radziszewski,[*,∥,†] Mark R. Nimlos,[*,∥,§] Paul R. Winter,[§] David C. Dayton,[∥] Donald E. David,[§,‡] and G. Barney Ellison[*,§]

Contribution from the Department of Chemistry and Biochemistry, University of Colorado, Boulder, Colorado 80309-0215, Integrated Instrument Design Facility, CIRES, University of Colorado, Boulder, Colorado 80309-0216, National Renewable Energy Laboratory, 1617 Cole Boulevard, Golden, Colorado 80401, and Department of Chemical Engineering and Petroleum Refining, Colorado School of Mines, Golden Colorado 80401
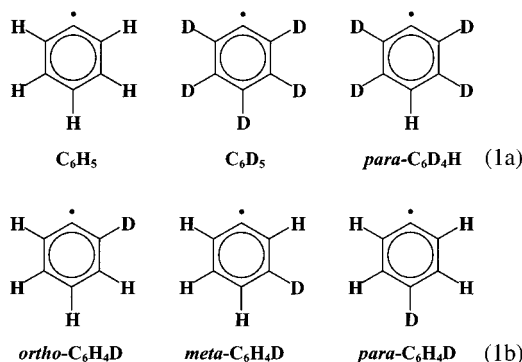
Received July 5, 2000

Abstract: We have measured the infrared absorption spectrum of C_6H_5, $\tilde{X}\,^2A_1$, in an Ar matrix at 10 K. The experimental frequencies (cm^{-1}) and polarizations follow. a_1 modes: 3086, 3072, 3037, 1581, 1441, 1154, 1027, 997, 976, 605; b_1 modes: 972, 874, 706, 657, 416; b_2 modes: 3071, 3060, 1624, 1432, 1321, 1283, 1159, 1063, and 587. Three different methods have been used for the production of the phenyl radicals. Infrared absorption spectra of five deuterated isotopomers, C_6D_5, $p\text{-}C_6H_4D$, $p\text{-}C_6HD_4$, $o\text{-}C_6H_4D$, and $m\text{-}C_6H_4D$, were recorded to compare experimental frequency shifts with calculated (UB3LYP/cc-pVDZ) harmonic frequency shifts. The use of CO_2 or NO as internal standards enabled the experimental determination of absolute infrared intensities. The linear dichroism was measured with photooriented samples to establish experimental polarizations of each vibrational band. True gas-phase vibrational frequencies were estimated by considering the gas-to-matrix shifts and matrix inhomogeneous line broadening. The phenyl radical matrix frequencies listed above are within ±1% of the gas-phase vibrational frequencies. The C_6H_5 frequencies from this paper supersede our earlier values reported in *J. Am. Chem. Soc.* **1996**, *118*, 7400−7401. See also: http://ellison.colorado.edu/phenyl.

I. Introduction

Benzene is the most perfect aromatic compound.[1−5] Because benzene is so stable, the radical derived from C_6H_6 by cleavage of a C−H bond is a reactive species. If benzene is the prototypical aromatic species that is encountered in many areas of pure chemistry,[6] combustion chemistry,[7−10] environmental chemistry[11] and biochemical problems,[12] then the C_6H_5 radical is an equally fundamental molecule. To characterize the structure and bonding of the phenyl radical, C_6H_5, we have measured

(a) the infrared absorption frequencies, (b) infrared polarizations, and (c) the infrared intensities for the following species:

$$C_6H_5 \qquad C_6D_5 \qquad para\text{-}C_6D_4H \qquad (1a)$$

$$ortho\text{-}C_6H_4D \qquad meta\text{-}C_6H_4D \qquad para\text{-}C_6H_4D \qquad (1b)$$

The phenyl radical, C_6H_5, is the prototypical aryl radical. Cleavage of the C−H bond in benzene, $D_0(C_6H_5\text{−H}) = 469 \pm 3$ kJ mol^{-1} (112.0 ± 0.6 kcal mol^{-1}), produces[13] this C_{2v} radical and an H atom. The infrared spectrum of C_6H_5, $\tilde{X}\,^2A_1$, has yet to be fully characterized. Pacansky *et al.* originally reported the matrix infrared absorption spectrum of phenyl radical measured by photodissociating benzoyl peroxide ($C_6H_5CO_2−OC(O)C_6H_5$) in an Ar matrix.[14−16] In a later study, several infrared absorptions were observed from the photolysis of nitro-

* Author for correspondence. E-mail: barney@jila.colorado.edu.
§ Department of Chemistry and Biochemistry, University of Colorado.
‡ Integrated Instrument Design Facility, CIRES, University of Colorado.
∥ National Renewable Energy Laboratory.
† Colorado School of Mines.
(1) Wheland, G. W. *Resonance in Organic Chemistry*; John Wiley & Sons: New York City, 1955.
(2) Salem, L. *Pi Electron Theory of Organic Chemistry*; W. A. Benjamain: New York City, 1962.
(3) Roberts, J. D.; Caserio, M. C. *Basic Principles of Organic Chemistry*, 2nd ed.; W. A. Benjamin, Inc.: Menlo Park, CA, 1977.
(4) Carroll, F. A. *Perspectives on Structure and Mechanism in Organic Chemistry*; Brooks/Cole Publishing Company: New York City, 1998.
(5) Berson, J. A. *Chemical Creativity*; Wiley−VCH: Weinheim, FRG, 1999.
(6) Kenttämaa, H. *J. Chem. Soc., Perkin Trans.* **1999**, *2*, 2233−2240.
(7) Frenklach, M.; Warnatz, J. *Combust. Sci. Technol.* **1987**, *51*, 265−283.
(8) Yu, T.; Lin, M. C. *J. Am. Chem. Soc.* **1994**, *116*, 9571−6.
(9) Park, J.; Dyakov, I. V.; Lin, M. C. *J. Phys. Chem. A* **1997**, *101*, 8839−8843.
(10) Marinov, N. M.; Pitz, W. J.; Westbrook, C. K.; Castaldi, M. J.; Senkan, S. M. *Combust. Sci. Technol.* **1996**, *116−117*, 211−287.
(11) Wallington, T. J.; Egsgaard, H.; Nielsen, O. J.; Platz, J.; Sehested, J.; Stein, T. *Chem. Phys. Lett.* **1998**, *290*, 363−370.
(12) Halliwell, B.; Gutteridge, J. M. C. *Free Radicals in Biology and Medicine,* 3rd ed.; Oxford University Press: New York City, 1999.

(13) Davico, G. E.; Bierbaum, V. M.; Depuy, C. H.; Ellison, G. B.; Squires, R. R. *J. Am. Chem. Soc.* **1995**, *117*, 2590−2599.
(14) Pacansky, J.; Bargon, J. *J. Am. Chem. Soc.* **1975**, *97*, 6896.
(15) Pacansky, J.; Gardini, G. P.; Bargon, J. *J. Am. Chem. Soc.* **1976**, *98*, 2665.
(16) Pacansky, J.; Brown, D. W. *J. Phys. Chem.* **1983**, *87*, 1553.

sobenzene (C_6H_5NO) in argon matrices.[17] Recently the frequencies, polarizations, and infrared intensities were reported for all 24 IR active transitions of C_6H_5 following photodissociation of benzoyl peroxide and benzoic anhydride in a cryogenic matrix.[18] The matrix-photodissociation products were observed to have an EPR spectrum that is identical to that of phenyl radical.[19] These C_6H_5 IR assignments[18] were based upon kinetic studies during photolysis and subsequent warm-up as well as agreement with the harmonic frequencies resulting from *ab initio* electronic structure calculations (UB3LYP/DZ95).

In addition to the vibrational spectrum of phenyl, the ultraviolet absorption spectrum of C_6H_5 has also been scrutinized.[11,20,21] Over the region $52,000-4,000$ cm^{-1}, three electronic transitions[22] have been assigned: $T_0[\tilde{A}\ ^2B_1 \leftarrow \tilde{X}\ ^2A_1] =$ 2.43 eV (510.5 nm, $\epsilon = 2.8$ L mol^{-1} cm^{-1}); $\lambda_{max}[\tilde{B}\ ^2A_1 \leftarrow \tilde{X}$ $^2A_1] = 5.27$ eV (235.1 nm, $\epsilon = 220$ L mol^{-1} cm^{-1}); $T_0[\tilde{C}\ ^2B_2$ $\leftarrow \tilde{X}\ ^2A_1] = 5.86$ eV (211.5 nm, $\epsilon = 1650$ L mol^{-1} cm^{-1}). As of yet there have been no reports of any microwave transitions for phenyl. Besides the excitation spectra of the C_6H_5 radical, the energetics for electron removal and addition have been measured. Following preparation by F atom reaction with benzene, the ionization potential of phenyl radical, $C_6H_5^+$ $\tilde{X}$ $^1A_1 \leftarrow C_6H_5$ $\tilde{X}$ $^2A_1$, has been estimated[23] to be 8.0 ± 0.1 eV. Negative ion photodetachment studies[24] of mass-selected beams of $C_6H_5^-$ have established the electron affinity of phenyl, C_6H_5 $\tilde{X}$ $^2A_1 \leftarrow C_6H_5^-$ $\tilde{X}$ $^1A_1$, as 1.096 ± 0.006 eV.

The reaction kinetics of the C_6H_5 radical with a wide variety of reactants have been investigated by cavity ringdown spectroscopy[25,26] and laser flash photolysis techniques.[27] The reaction kinetics[8,9,28,29] of phenyl with the diatomics: HBr, O_2, NO, and H_2, have been reported. Further studies of C_6H_5 with carbon tetrachloride,[29,30] ethylene,[31] methane,[32] benzene,[33] acetylene,[34] and toluene[35] have been published.

(17) Hatton, W. G.; Hacker, N. P.; Kasai, P. H. *J. Chem. Soc., Chem. Commun.* **1990**, 227−229.

(18) Radziszewski, J. G.; Nimlos, M. R.; Winter, P. R.; Ellison, G. B. *J. Am. Chem. Soc.* **1996**, *118*, 7400−7401.

(19) Kasai, P. H.; Hedaya, E.; Whipple, E. B. *J. Am. Chem. Soc.* **1969**, *91*, 4364.

(20) Engert, J. M.; Dick, B. *Appl. Phys. B: Lasers Opt.* **1996**, *B63*, 531−535.

(21) Radziszewski, J. G. *Chem. Phys. Lett.* **1999**, *301*, 565−570.

(22) The lowest optically excited state of C_6H_5 arises from excitation of a low-lying π electron to the σ nonbonding orbital. By analogy to benzene, phenyl radical will have three pairs of π electrons $\{1b_1, 2b_1, 1a_2\}$ and a nonbonding electron $\{a_1\}$. Consequently the $\tilde{A}$ $^2B_1$ state of C_6H_5 at 2.43 eV arises from: $|1b_1^2 2b_1^1 1a_2^2\ a_1^2\rangle \leftarrow |1b_1^2 2b_1^2 1a_2^2\ a_1^1\rangle$. This implies that there will be another electronic state of phenyl near the 510 nm band that is very weak. An excited state of C_6H_5 near 2.4 eV will arise from excitation from the other HOMO and will produce a $^2A_2$ state of C_6H_5 $|1b_1^2\ 2b_1^2 1a_2^1$ $a_1^2\rangle \leftarrow |1b_1^2 2b_1^2\ 1a_2^2\ a_1^1\rangle$. Since a transition to a $^2A_2$ state of C_6H_5 is dipole-forbidden, this low-lying phenyl state has yet to be detected.

(23) Butcher, V.; Costa, M. L.; Dyke, J. M.; Ellis, A. R.; Morris, J. A. *Chem. Phys.* **1987**, *115*, 261.

(24) Gunion, R.; Gilles, M.; Polak, M.; Lineberger, W. C. *Int. J. Mass Spectrom. Ion Processes* **1992**, *117*, 601.

(25) Yu, T.; Lin, M. C. *J. Am. Chem. Soc.* **1993**, *115*, 4371−4372.

(26) Brioukov, M. G.; Park, J.; Lin, M. C. *Int. J. Chem. Kinet.* **1999**, *31*, 577−582.

(27) Scaiano, J. C.; Stewart, L. C. *J. Am. Chem. Soc.* **1983**, *105*, 3609−3614.

(28) Lin, M. C.; Yu, T. *Int. J. Chem. Kinet.* **1993**, *25*, 875−80.

(29) Yu, T.; Lin, M. C. *J. Phys. Chem.* **1994**, *98*, 2105−2109.

(30) Yu, T.; Lin, M. C. *J. Phys. Chem.* **1995**, *99*, 8599−8603.

(31) Yu, T.; Lin, M. C. *Combust. Flame* **1995**, *100*, 169−176.

(32) Tokmakov, I. V.; Park, J.; Gheyas, S.; Lin, M. C. *J. Phys. Chem. A* **1999**, *103*, 3636−3645.

(33) Park, J.; Burova, S.; Rodgers, A. S.; Lin, M. C. *J. Phys. Chem. A* **1999**, *103*, 9036−9041.

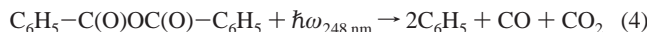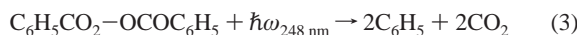(34) Yu, T.; Lin, M. C.; Melius, C. F. *Int. J. Chem. Kinet.* **1994**, *26*, 1095−1104.

(35) Park, J.; Chakraborty, D.; Bhusari, D. M.; Lin, M. C. *J. Phys. Chem. A* **1999**, *103*, 4002−4008.

We have completed an extensive study of the IR absorption spectra of the C_6H_5 radical and several isotopically labeled isomers that have been isolated in cryogenic matrices. We report a complete set of vibrational frequencies for the C_6H_5 radical, $\{\nu\}_i$, and, in addition, we have measured the polarizations of each of the bands as well as the intensities of the IR modes, $\{A\}_i$. Because of our examination of six different C_6H_5 isotopomers, new polarization measurements, and the development of an intense hyperthermal source of C_6H_5 radicals, the frequencies and intensities of the phenyl radical in this paper supersede our earlier data set published in 1996.[18]
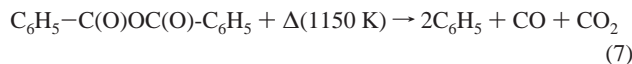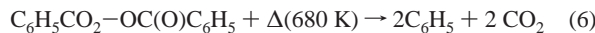
II. Experimental Section

We have prepared the phenyl radical in Ar matrices from four different precursors (see below) and by using three different techniques, (a) photodissociation of precursors trapped in noble gas matrices, (b) vacuum pyrolysis in an effusive thermal source, and (c) flash pyrolysis in a hyperthermal nozzle followed by supersonic jet expansion. In the following discussion these three methods will be presented in detail. The general techniques of matrix isolation of reactive intermediates are well-known and described elsewhere.[36−39] For all matrix isolation experiments, a two-stage, closed-cycle, He-cryostat (APD Cryogenics) was used for cooling a 5 mm thick CsI window to 10 ± 0.5 K. The cryostat pressure was kept at 2.7×10^{-6} mbar (2×10^{-6} Torr), or lower, during cooling.

Preparation of Phenyl Radical. (a) Photodissociation of Matrix Isolated Precursors. Phenyl radical can be prepared in high yields by photodissociation of nitrosobenzene, C_6H_5NO (eq 2), or benzoyl peroxide, $C_6H_5CO_2-OCOC_6H_5$ (eq 3), when trapped in an Ar matrix (1:1000) at 10 K. Lower yields of C_6H_5 can be formed by the irradiation of benzoic anhydride, $C_6H_5-C(O)OC(O)-C_6H_5$ (eq 4) and phenyl iodide, C_6H_5I (eq 5). Because of the ease of their preparation, most of the precursors that we used for this study were the aryl iodides.

$$C_6H_5NO + \hbar\omega_{308\,nm} \rightarrow C_6H_5 + NO \tag{2}$$

$$C_6H_5CO_2-OCOC_6H_5 + \hbar\omega_{248\,nm} \rightarrow 2C_6H_5 + 2CO_2 \tag{3}$$

$$C_6H_5-C(O)OC(O)-C_6H_5 + \hbar\omega_{248\,nm} \rightarrow 2C_6H_5 + CO + CO_2 \tag{4}$$

$$C_6H_5I + \hbar\omega_{248\,nm} \rightarrow C_6H_5 + I \tag{5}$$

The laser light source used in eqs $2-5$ was a pulsed excimer laser (Lambda Physik) generating 193 nm (ArF) or 248 nm (KrF) photons, or an excimer laser (Lumonics) generating 308 nm (XeC*l*) photons. For polarization experiments (see below), we have used a Glan-Thompson polarizer (Oriel) for the excimer laser source and a wire grid polarizer (KRS-5, Cambridge Physics) for the linear dichroism infrared absorption spectra.

(b) Vacuum Pyrolysis in an Effusive Thermal Source. Phenyl radical can also be prepared in high yields by vacuum pyrolysis in an effusive thermal source of benzoyl peroxide (eq 6) or benzoic anhydride (eq 7)

$$C_6H_5CO_2-OC(O)C_6H_5 + \Delta(680\ K) \rightarrow 2C_6H_5 + 2\ CO_2 \tag{6}$$

$$C_6H_5-C(O)OC(O)-C_6H_5 + \Delta(1150\ K) \rightarrow 2C_6H_5 + CO + CO_2 \tag{7}$$

In our pyrolysis oven, which we can use with temperatures up to 1500 K, we can change the length of the hot zone. The heating element was wrapped around a quartz tube, i.d. 10 mm, 30 mm in length. Argon gas containing precursor in a ca. $\sim$1:100 ratio flows through the tube

(36) Hallam, H. E. *Vibrational Spectroscopy Of Trapped Species*; J. Wiley: New York, 1973.

(37) Meyer, B. *Low-Temperature Spectroscopy*; Elsevier: New York, 1971.

(38) Norman, I.; Porter, G. *Nature* **1954**, *174*, 508.

(39) Whittle, E.; Dows, D. A.; Pimentel, G. C. *J. Chem. Phys.* **1954**, *22*, 1943.
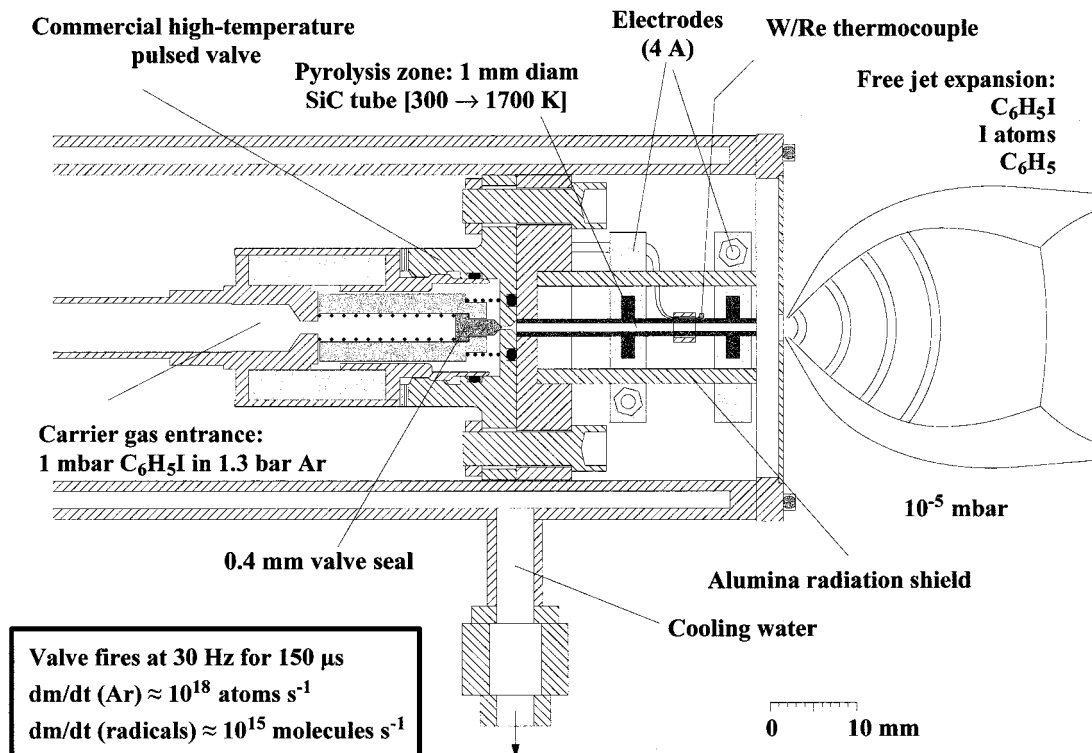
IR Spectrum of the Matrix-Isolated Phenyl Radical

J. Am. Chem. Soc., Vol. 123, No. 9, 2001   1979

Commercial high-temperature pulsed valve

Pyrolysis zone: 1 mm diam SiC tube [300 → 1700 K]

Electrodes (4 A)

W/Re thermocouple

Free jet expansion:
C_6H_5I
I atoms
C_6H_5

Carrier gas entrance:
1 mbar C_6H_5I in 1.3 bar Ar

0.4 mm valve seal

10^{-5} mbar

Alumina radiation shield

Cooling water

Valve fires at 30 Hz for 150 μs
dm/dt (Ar) $\approx 10^{18}$ atoms s^{-1}
dm/dt (radicals) $\approx 10^{15}$ molecules s^{-1}

0   10 mm

Figure 1. Hyperthermal nozzle for flash pyrolysis of a precursor in a pulsed gas mixture of precursor/carrier gas (see text).

directly into the matrix chamber. The experiment is performed inside an FTIR spectrometer, which allows continuous monitoring of the reaction progress.

While this technique works well with the peroxide and anhydride precursors, the phenyl radical yield is poor for both C_6H_5I and C_6H_5-NO precursors. The reasons for this are not obvious and should be sought in a careful study of the kinetics and dynamics of the pyrolysis reactions and competing side-reactions such as disproportionation and recombination. A contributing factor might be the spatial separation of the two formed phenyl radicals by two CO_2 molecules in eq 6 and one CO_2 and one CO molecule in eq 7, which is likely to decrease the probability of both disproportionation and recombination.

A general problem in a vacuum pyrolysis is the long residence times (tens of milliseconds) in the effusive source. This makes it difficult to suppress side-reactions. Even in the cases of eqs 6 and 7, products from side-reactions obscures the spectra of the trapped products and makes analysis and assignments nontrivial.

(c) Flash Pyrolysis and Supersonic Expansion. A hyperthermal pulsed nozzle design for the production of jet-cooled organic reactive intermediates by flash pyrolysis, for example:

$$C_6H_5I + \Delta(1300 \text{ K}, 100\,\mu\text{s}) \rightarrow C_6H_5 + I \qquad (8)$$
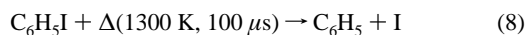
has been developed for the generation of high number densities of radicals.[40-48] We have adopted Chen's design[46] with modifications (Figure 1) for two identical pyrolysis ovens, one interfaced with a reflectron photoionization time-of-flight mass spectrometer (TOF) and

the other with a cryostat for matrix isolation and subsequent FTIR measurements. The TOF apparatus is used prior to matrix isolation of the desired radical in order to optimize all nozzle parameters. This combination of techniques has turned out to be the most successful for the production and detection of C_6H_5, as well as other reactive intermediates in our laboratory, and will be described in some detail here.

The heart of our nozzle (Figure 1) is a 28 mm long SiC tube (Hexaloy SA high density SiC, Carborundum Corp.) with i.d. 1 mm and o.d. 2 mm, which is resistively heated to temperatures up to 1700 K. Silicon carbide has a high[49] dielectric constant ($\epsilon = 10.2$), high[49] thermal conductivity ($k = 0.42$ W cm^{-1} K^{-1}), and an inverted temperature coefficient of resistance, which makes it ideal for high current throughput (4 A) and high-temperature conditions. The tube is based in, and extends through, a 6 mm thick circular copper plate ($\varnothing$ 36 mm), which acts as a heat sink between the hot tube and the solenoid valve. A groove in the copper plate supports an alumina cylinder, which serves two purposes: it acts as a radiation shield in the radial direction from the SiC tube, and it supports two Mo electrodes in slits concentric with and parallel to the SiC tube. The electrodes each hold a hollow graphite disk which makes a tight fit around the SiC tube. Gauge 18 copper wire (not shown) connects the high current (4 A) source to and from the electrodes. A 2 mm long alumina sleeve holds a high-temperature W/Re (Omega) thermocouple in place and in thermal contact with the outer surface of the SiC tube. The distance between the two electrodes is 10 $\pm$ 2 mm. Heating and temperature control is accomplished by a microprocessor-based temperature controller (Love Controls, series 16A, Dwyer Instruments)

The copper plate is bolted to a stainless steel faceplate of a high-temperature solenoid pulsed valve (General Valve, series 9). Holes are bored through both plates to accommodate wire feed-throughs. High-temperature fluoro-elastomer O-rings (Kalrez, Dupont) seal between the faceplate and the copper plate, and between the faceplate and valve body. The whole assembly is mounted inside a vacuum-sealed stainless steel cylinder (i.d. 35 mm, o.d. 45 mm) with a hollow wall for water cooling. The cylinder (and thus the SiC tube) is evacuated to 10^{-6} mbar through the exit end of the cylinder (right-most end in Figure 1). This end is mounted to a photoionization vacuum chamber in our TOF

(40) Chen, P.; Colson, S. D.; Chupka, W. A.; Berson, J. A. *J. Phys. Chem.* **1986**, *90*, 2319.

(41) Chen, P.; Colson, S. D.; Chupka, W. A. *Chem. Phys. Lett.* **1988**, *147*, 466.

(42) Blush, J. A. *J. Am. Chem. Soc.* **1989**, *111*, 8951.

(43) Clauberg, H.; Minsek, D. W.; Chen, P. *J. Am. Chem. Soc.* **1992**, *114*, 99.

(44) Minsek, D. W.; Blush, J. A.; Chen, P. *J. Phys. Chem.* **1992**, *96*, 2025.

(45) Minsek, D. W.; Chen, P. *J. Phys. Chem.* **1990**, *94*, 8399.

(46) Kohn, D. W.; Clauberg, H.; Chen, P. *Rev. Sci. Instrum.* **1992**, *63*, 4003.

(47) Zhang, X.; Chen, P. *J. Am. Chem. Soc.* **1992**, *114*, 3147.

(48) Rohrs, H. W.; Wickham-Jones, C. T.; Berry, D.; Ellison, G. B.; Argrow, B. M. *Rev. Sci. Instrum.* **1995**, *66*, 2430.

(49) *Handbook of Chemistry and Physics*, 73rd ed.; Lide, D. R., Ed.; CRC: Boca Raton, 1992.

Table 1. Calculated Fluid Properties for Flow through a Narrow SiC Tube Heated to 1300 K

flow property	tube inlet	tube exit	at matrix window
temperature/K	300	1000	4
pressure/bar	0.5	0.2	$<10^{-9}$
flux (total)/s^{-1}	3.5×10^{18}	3.5×10^{18}	$1.2 - 2.5 \times 10^{18}$
flux (radicals)/s^{-1}	2.1×10^{15}	2.1×10^{15}	$0.7 - 1.5 \times 10^{15}$
flow speed/mach number	0.2	1	27
flow speed/cm s^{-1}	7×10^3	6×10^4	2×10^6
time in hot zone/s	0	10^{-4}	–

experiments, or to a cryostat vacuum-shroud in our matrix isolation experiments. In both cases, the exit of the nozzle faces a vacuum of about 10^{-6} mbar, which creates a free-jet expansion of the pyrolysis products. This ensures rapid cooling and isolation of the radicals in the gas-phase.

From a 1 L gas reservoir, a gas mixture of approximately 0.06% C_6H_5I in Ar is fed through the valve with a stagnation pressure of 1.0– 1.3 bar. Typically we operate the valve at 10–50 Hz with pulse widths in the range 150–300 μs. During this opening time, the gas pulse enters the beginning of the SiC tube through a 0.4 mm orifice in the center of the faceplate, expands into the 28 mm long, 1.0 mm wide, hot SiC tube, and in turn into the vacuum by the exit of the nozzle.

The fluid dynamics of the Ar gas in the hyperthermal nozzle can be described as a compressible flow through a heated capillary, fed by a converging–diverging nozzle. This problem has been well-studied,[50-52] in particular by Chen[53] whose work has provided inspiration for the design of our current hyperthermal nozzle. A detailed treatment of the operational characteristics of our nozzle will be presented elsewhere.[54] Table 1 summarizes some important results.

(D) Photoionization Mass Spectrometry. Prior to matrix deposition, the optimal parameters for clean radical production in the hyperthermal nozzle are found by monitoring pyrolysis products in a TOF mass spectrometer. This instrument has been described earlier.[55-57] Briefly, the pulsed (10 Hz, 125 μs), ionizing (118.2 nm or 10.487 eV) laser beam is generated by frequency tripling of the third harmonic (354.6 nm, 55 mJ/pulse) of a Nd:YAG laser. The tripling cell had a 4 Torr Xe/940 Torr Ar gas mixture. The effluent from the hyperthermal nozzle is skimmed, forming a molecular beam orthogonal to the laser beam. The molecular beam pulse is triggered by, and in phase with, the laser pulses. After ionization of species in the molecular beam that have IP < 10.487 eV, the ions are injected by a repeller plate into the flight tube by appropriate ion optics and accelerated into the drift zone by a strong electric field (860 V). At the end of the flight tube, the ions are re-grouped and reflected (by a small angle) by a series of grids down to a microchannel plate detector at the base of the flight tube. The flight tube is kept at vacuum (10^{-7} mbar) by a turbomolecular pump.

The relation between flight time, t, and ion mass, m, is[56,57]

$$t = \left\{ \frac{\sqrt{2}(\sqrt{U_0 + qEs_a} \pm \sqrt{U_0})}{qE} + \frac{D\sqrt{2}}{2\sqrt{U_0 + qEs_a}} \right\} \sqrt{m} \quad (9)$$

where U_0 is the initial ion translational energy, q the charge, E the electric field strength, s_a the average distance traveled in the accelerating field, and D the drift distance. Before exposure to the decomposition products from the hyperthermal nozzle, the TOF is calibrated with CH_2-

(50) Anderson, J. D., Jr. *Modern Compressible Flow with Historic Perspective*; McGraw-Hill Book Company: New York City, 1982.

(51) Daneshyar, H. *One-Dimensional Compressible Flow*; Pergamon Press: New York City, 1976.

(52) Shapiro, A. H. *The Dynamics and Thermodynamics of Compressible Flow*; Robert, E., Ed.; Krieger Publishing Company: Malabar, 1985.

(53) Chen, P. *The Spectroscopy and Photochemistry of Free Radicals in a Supersonic Jet.* Ph.D. Thesis, Yale University, 1987.

(54) Friderichsen, A. V.; Nimlos, M. R.; David, D. E.; Ellison, G. B. In progress.

(55) Mamyrin, B. A.; Krataev, V. I.; Shmikk, D. V.; Zagulin, V. A. *Zh. Eksp. Teor. Fiz.* **1973**, *64*, 82–89.

(56) Guilhaus, M. *J. Mass. Spectrom.* **1995**, *30*, 1519–1532.

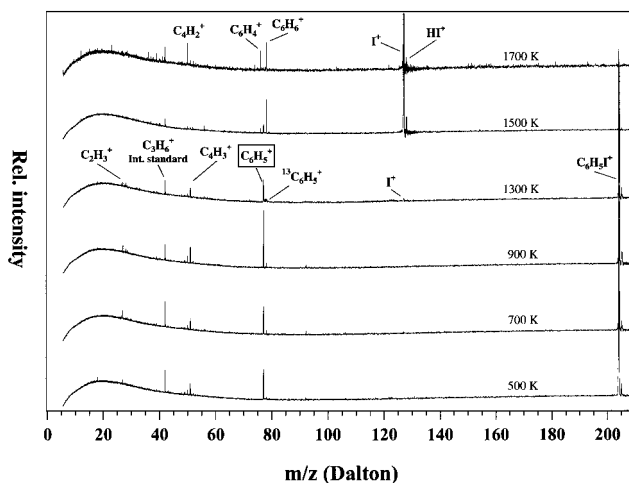(57) Wiley, W. C.; McLaren, I. H. *Rev. Sci. Instrum.* **1955**, *26*, 1150–1157.

Figure 2. Photoionization time-of-flight mass spectra of flash-pyrolyzed iodobenzene as a function of nozzle temperature. At nozzle temperatures too low for thermal decomposition, the $C_6H_5^+$ can still be detected. This can happen if the parent compound ion ($C_6H_5I^+$) is unstable and decomposes into the radical ion ($C_6H_5^+$) and a neutral leaving group (iodine). The instability of $C_6H_5I^+$ arises from the vibrational excitation added to the precursor iodobenzene in the hot nozzle. Since vibrational energy is difficult to quench in a free expansion, the vibrational energy plus the excess photon energy after photoionization can be sufficient to overcome the dissociation barrier. At pyrolysis temperatures, one observes both phenyl radical and iodine cation. At temperatures higher than 1300 K, the peak at *m/z* 77 Da splits into a doublet at *m/z* 76 and 78 Da, respectively, suggesting formation of benzyne, C_6H_4, and benzene, C_6H_6.

$CHCH_3$ (*m/z* 42), or other simple hydrocarbon mixed with an inert gas. This provides a straightforward calibration between the measured flight time and ion mass. The parameters of the hyperthermal nozzle are then adjusted to the point where only the desired radical ion and leaving group ion (e.g., I^+) are detected. These parameters include sample temperature, valve temperature, nozzle temperature, pulse duration, and stagnation pressure of carrier gas.

Caution must be used in interpreting the time-of-flight mass spectrum. At nozzle temperatures too low for thermal decomposition but above ambient temperature, the radical ion can still be detected. This can happen if the parent compound ion is unstable and decomposes into the radical ion and a neutral leaving group:

$$C_6H_5I + \hbar\omega_{118.2\,nm} \rightarrow [C_6H_5I^+]^* + e^- \rightarrow C_6H_5^+ + I + e^- \quad (10)$$
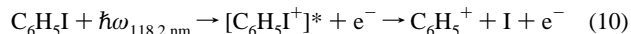
The instability of $C_6H_5I^+$ arises from the vibrational excitation imparted to the precursor, iodobenzene, in the hot nozzle. Since vibrational energy is difficult to quench in a free expansion, the vibrational energy plus the excess photon energy after photoionization can be sufficient to overcome the dissociation barrier. The ionization potential of C_6H_5I is measured[58] to be 8.72 eV. Thus, the ionizing laser photons leaves ~1.8 eV excess energy after ionization. Adding this energy to a vibrationally excited precursor could be sufficient to overcome the dissociation barrier, $D_0(C_6H_5{-}I) = 264 \pm 3$ kJ mol^{-1} [63 $\pm$ 0.8 kcal mol^{-1} = 2.74 eV].[13,59]

At the C_6H_5I pyrolysis temperature one observes both phenyl radical and iodine cation:

$$C_6H_5I + \Delta(1300\,K) \rightarrow C_6H_5 + I\,[+\,\hbar\omega_{118.2\,nm}] \rightarrow$$
$$[C_6H_5]^+ + I^+ + 2e^- \quad (11)$$
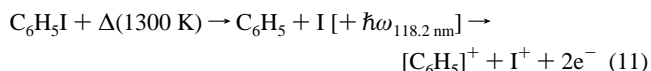
This is illustrated in Figure 2, which shows the TOF spectra of

(58) Lias, S. G.; Bartmess, J. E.; Liebman, J. F.; Holmes, J. L.; Levin, R. D.; Mallard, W. G. *J. Phys. Chem. Ref. Data* **1988**, *17* (supplement 1), 1.

(59) Pedley, J. B.; Naylor, R. D.; Kirby, S. P. *Thermochemistry of Organic Compounds*, 2nd ed.; Chapman and Hall: New York, 1986.

iodobenzene after pyrolysis at different temperatures. At temperatures below 1300 K, the mass signal of $C_6H_5^+$ (m/z 77 Da) is detected, but I^+ (m/z 126.9 Da) is absent. At temperatures above 1300 K, both signals of $C_6H_5^+$ and I^+ are detected. This is an indication that the temperature is high enough to fracture the C_6H_5-I bond and thus the minimum pyrolysis temperature we need for our matrix experiments. At temperatures higher than 1300 K, the peak at m/z 77 Da splits into a doublet at m/z 76 and 78 Da, respectively, suggesting formation of benzyne, C_6H_4, and benzene, C_6H_6.

Interestingly, the mass signal at m/z 77 Da is present even at 500 K. Can vibrational excitation plus excess photoionization energy account for the dissociation of C_6H_5I at this temperature? Treating the normal modes in C_6H_5I as harmonic oscillators, obeying a Boltzmann distribution of excited vibrational states (to $v = 1$, 2 and 3), the vibrational excitation energy contribution to the internal energy at 500 K is about 25 kJ mol^{-1}. The rotational energy, $^3/_2RT$, is 6.2 kJ mol^{-1}. Adding these to the excess photon energy (1.8 eV = 174 kJ mol^{-1}) gives a total of 204 kJ mol^{-1}, which is 3/4 of the bond dissociation barrier, $D_0(C_6H_5-I) = 264 \pm 3$ kJ mol^{-1}. Bearing in mind that the Boltzmann distribution has a tail of populations excited to higher energies, it does not seem unlikely that the dissociation of C_6H_5I from excess photoionization energy is triggered by vibrational excitation.

One other possibility is the absorption of nonfocused 355 nm photons from the 3rd harmonic of the Nd:YAG laser. This energy (337 kJ mol^{-1}) would certainly be sufficient to dissociate C_6H_5I. However, the molar extinction coefficient of C_6H_5I at this wavelength is vanishing.[60]

Matrix IR Spectroscopy. Mid and far-infrared spectra were recorded with a Nicolet Magna 550 or a Bruker Vectra 33 FTIR spectrometer, using a liquid N_2 cooled MCT detector type A (4000$-$600 cm^{-1}, $D^* = 5 \times 10^{10}$ cm Hz$^{1/2}$ W^{-1}) or B (4000$-$400 cm^{-1}, $D^* = 5 \times 10^9$ cm Hz$^{1/2}$ W^{-1}) in combination with a KBr beam splitter. For measurements below 400 cm^{-1} (4000$-$300 cm^{-1}), a DTGS detector ($D^* = 2 \times 10^8$ cm Hz$^{1/2}$ W^{-1}) with a CsI beam splitter was used. The resolution of all spectra was 0.125 cm^{-1}, except from the spectra recorded with the Bruker FTIR spectrometer, where the maximum resolution was 0.35 cm^{-1}. Both spectrometers were purged with N_2 or dry air.

Absolute Intensities. In addition to the vibrational frequencies ($\tilde{\nu}$) of the phenyl radical, it is important to measure the infrared intensities, A. Recall[61] that A is measured in the units of km mole^{-1} and is defined:

$$A = \int_{IR\,band} d\tilde{\nu}\,\sigma(\tilde{\nu}) = \frac{1}{nz}\int_{IR\,band} d\tilde{\nu}\,\ln\left|\frac{I_0}{I}\right| \qquad (12)$$

The photodissociation schemes for the production of C_6H_5 in eqs 2, 3, and 4 produce a leaving group that can act as an internal standard for the measurement of absolute intensities for all phenyl radical IR bands, provided the absolute intensity of the leaving group is known. In eq 3, one CO_2 molecule is produced for each C_6H_5. The absolute cross sections of CO_2 has been measured in an Ar matrix at 10 K by Radziszewski et al.[62] Thus, after correction of a small initial CO_2 contamination,[18] we can extract the absolute integrated intensities of phenyl radical, $A(C_6H_5)$, using

$$A(C_6H_5) = A(CO_2)\frac{\int_{C_6H_5} d\tilde{\nu}[OD]}{\int_{CO_2} d\tilde{\nu}[OD]} \qquad (13)$$

where the integrals are the actual measured intensities, integrated over the infrared band, and OD is the optical density, $OD(\tilde{\nu}) = \log_{10}[I_0(\tilde{\nu})/I(\tilde{\nu})]$.

Polarization Studies. Experimental determinations of transition dipole moment directions are useful whenever spectral assignments are attempted.[63-67] When photochemical transformations are performed with polarized light in a highly viscous environment, free of molecular rotation, such as a noble gas at 10 K, and the photochemical conversion of precursor is only partial, both precursor and product molecules become partially photooriented. Photoorientation is a consequence of photoselection: The probability of photon absorption and, thus, effective yield of photochemical transformation in any particular macroscopic direction is proportional to the quantity $\langle\cos^2(\mathbf{M}, \mathbf{E})\rangle$, where $(\mathbf{M}, \mathbf{E})$ is the angle between the electronic transition dipole moment $\mathbf{M}$ and the electric field vector, $\mathbf{E}$, of the light. The brackets indicate spatial averaging over all molecules. For example, if the transition dipole moment of the transition leading to photodissociation is parallel to a molecular axis u in the precursor molecules, molecules in which the angle between u and the plane of polarization, Z, is small, have the highest probability of photochemical conversion.

Photoselection produces spatially anisotropic ensembles of precursor and photoproduct molecules and subsequent linear dichroism (LD) measurements, for example, two linear independent polarized IR spectra, yield information on vibrational symmetries and transition dipole moment directions: The absorption intensity measured along Z, after a partial conversion, will be lower than measured along direction Y perpendicular to it, for all transitions proceeding along u, that is $E_Z - E_Y < 0$ (negative dichroism). For transitions proceeding in directions perpendicular to u, $E_Z - E_Y > 0$ (positive dichroism).

For molecules belonging to high-symmetry point groups, such as C_{2v}, D_{2h}, or D_{6h}, the transition for any electric dipole absorption, or emission, process will be restricted to proceed along either one of the three principal molecular axes, x, y, or z. As a consequence, two independent photoorientation experiments will reveal the absolute symmetry of any absorption (or emission) band, if the symmetries of the two electronically excited states are known and not identical. This situation is favored for C_6H_5, C_6H_5I, and C_6H_5NO, which have electronically excited states that can be easily populated with an excimer laser line of the right wavelength.[18,21]

In our photoorientation experiments we have photoselected either the precursor C_6H_5I (and produced C_6H_5), or the product C_6H_5 (thus destroying the radical). In the first case, we obtain anisotropic ensembles of C_6H_5I and C_6H_5, in the second case anisotropic ensembles of C_6H_5 and photofragmentation products.

We have used four different polarized wavelengths for exciting into different states in C_6H_5, C_6H_5I, $C_6H_5CO_2-OCOC_6H_5$, or C_6H_5NO: 193 nm (into a B_2 state), 248 or 266 nm (into an A_1 state) to create or destroy phenyl radical from iodo or peroxy precursors, or 308 nm to produce partially oriented samples of phenyl radical from nitrosobenzene.

Irradiating C_6H_5 with 248 nm light excites the radical into the second excited state, $\lambda_{max}[\tilde{B}\ ^2A_1 \leftarrow \tilde{X}\ ^2A_1] = 5.27$ eV (235.1 nm) from which it dissociates. Since the ground state is totally symmetric ($^2A_1$), the transition dipole moment will be of symmetry $A_1 \otimes A_1 = A_1$. In C_6H_5, this moment will transform like the z molecular axis under the C_{2v} point group (parallel to the C_2 axis). In an isotropic ensemble of C_6H_5, molecules whose z axes align best with the electric field vector of the plane polarized laser light, will be preferentially excited, and destroyed. A subsequent measurement of the IR linear dichroism will exhibit a negative dichroism for all vibrations of a_1 symmetry. The remaining vibrations of b_1 and b_2 symmetry will exhibit positive dichroism; for a discussion of all aspects of these selection rules see the monograph of Michl and Thulstrup.[66]

If the ensemble of phenyl radicals is irradiated with 193 nm light, C_6H_5 will be excited into the third excited-state $T_0[\tilde{C}\ ^2B_2 \leftarrow \tilde{X}\ ^2A_1] = 5.86$ eV (211.5 nm) where it predissociates. In this case the transition dipole moment is of B_2 symmetry and the IR linear dichroism will be negative for all vibrations of b_2 symmetry, while the linear dichroism of vibrations of a_1 and b_1 symmetry will be positive.

The obtained linear dichroism spectra allow us to distinguish between all three vibrational symmetry species a_1, b_1, and b_2 (see Figure 6),

(60) Johnson, E. A. In *UV Atlas of Organic Compounds*; Plenum Press: New York, 1966; Vol. 2.

(61) Pugh, L. A.; Narahari Rao, K. In *Molecular Spectroscopy: Modern Research*; Rao, K. N., Ed.; Academic Press: New York, 1976; Vol. II, pp 165−227.

(62) Radziszewski, J. G.; Hess, B. A., Jr.; Zahradnik, R. *J. Am. Chem. Soc.* **1992**, *114*, 52.

(63) Albrecht, A. C. *J. Mol. Chem.* **1961**, *6*, 84.

(64) Johnson, P. M.; Albrecht, A. C. *J. Chem. Phys.* **1968**, *48*, 851.

(65) Johnson, P. M. *J. Chem. Phys.* **1970**, *52*, 5745.

(66) Michl, J.; Thulstrup, E. W. *Spectroscopy with Polarized Light. Solute Alignment by Photoselection in Liquid Crystals, Polymers, and Membranes*; VCH Publishers: Deerfield Beach, FL, 1986.

(67) Thulstrup, E. W.; Michl, J. *Elementary Polarization Spectroscopy*; VCH Publishers: New York City, 1989.
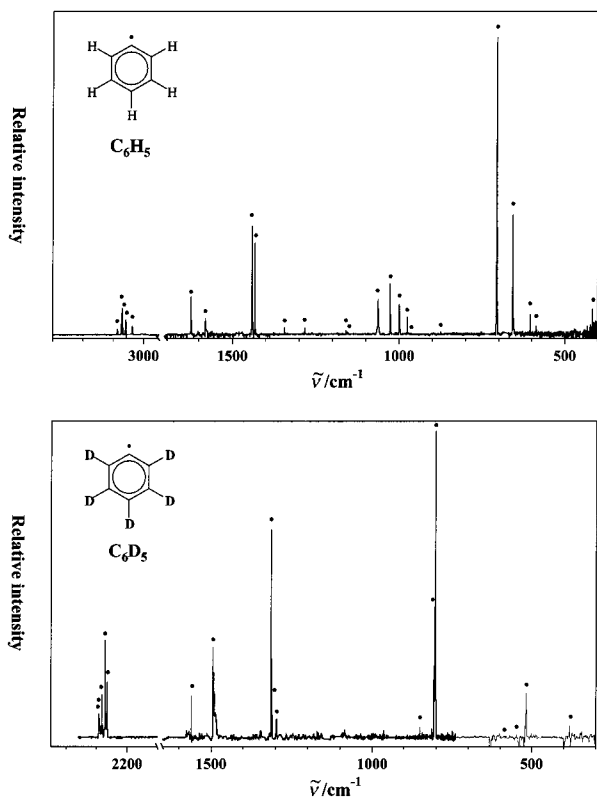
Figure 3. Infrared spectra of C_6H_5 (top) and C_6D_5 (bottom). The spectrum of C_6H_5 was measured on an Ar matrix at 10 K, containing products from flash-pyrolyzed C_6H_5I. Precursor bands and bands from the side-product C_6H_6 are subtracted. The precursor/Ar ratio was 0.06%. Experimental spectra of C_6D_5 were obtained from matrix-isolated and -photolyzed $C_6D_5CO_2$–$OCOC_6D_5$, C_6D_5NO, and C_6D_5I. Peaks assigned to fundamentals are annotated (●). See also Tables 2 and 3.

because transitions along the corresponding molecular axes (*x*, *y*, or *z*) show different patterns of dichroism changes:

	a_1	b_1	b_2
$\hbar\omega$ (248 nm, A_1)	−	+	+
$\hbar\omega$ (193 nm, B_2)	+	+	−

Annealing Experiments. When applying eq 2 or 5, an additional proof for the formation of C_6H_5, comes from a gentle, and short, warm-up of the matrix to about 45 K, followed by re-cooling to 10 K. This annealing allows the photodecomposed products, which will only be a few angstroms apart, to recombine. A subsequent FTIR measurement of the absorption spectrum will reveal a decrease in radical peak intensity and an increase in precursor or biphenyl, C_6H_5–C_6H_5, peak intensities.

III. Results and Discussion

Figures 3–5 show the infrared spectra of C_6H_5 and five isotopomers, C_6D_5, p-C_6H_4D, p-C_6HD_4, o-C_6H_4D, and m-C_6H_4D. The C–H stretches are shown only for C_6H_5 and C_6D_5, for which three different phenyl radical precursors were used. The remaining isotopomers were prepared exclusively from the corresponding iodobenzenes and a safe spectral assignment in this region could not be justified due to strong perturbations of the C–H stretching vibrational energy levels from iodine in the matrix. Figure 6 shows the linear dichroism of ν_{16} (706 cm^{-1}, b_1), ν_{22} (1432 cm^{-1}, b_2), and ν_5 (1441 cm^{-1}, a_1) in C_6H_5 after photoorientation by destruction of the radical with either 193 or 248 nm polarized light, and the linear dichroism of the same modes after photoorientation of C_6H_5 by photolysis of C_6H_5I with 248 nm polarized light. In the latter case we excite C_6H_5I into a $^1A_1$ electronic state, from which it predissociates. This
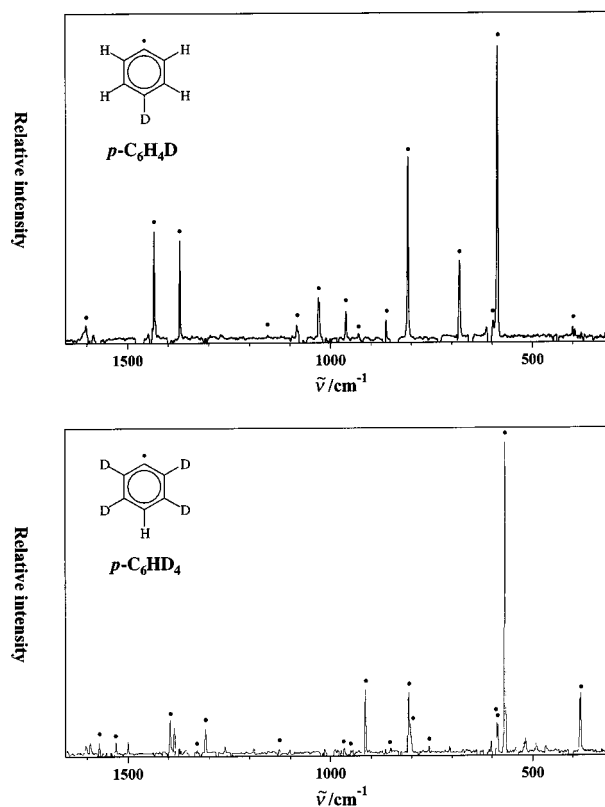

Figure 4. Infrared spectra of p-C_6H_4D (top) and p-C_6HD_4 (bottom). The spectra were obtained from matrix-isolated and -photolyzed, deuterated phenyl iodides. Peaks assigned to fundamentals are annotated (●). See also Tables 4 and 5.

causes the ensemble of C_6H_5I to be partially depleted for molecules having their C_2 axis oriented with small angles to the electric field vector of the 248 nm polarized laser beam. This, in turn, implies that the ensemble of photolysis products, C_6H_5, will have an average orientation with the C_2 axis aligned with a relatively small angle to the electric field vector of the polarizing light. A subsequent linear dichroism measurement will show a negative LD for all b_1 vibrations, and a positive LD for a_1 and b_2.

Tables 2–7 summarize our experimental findings in terms of vibrational frequencies and intensities. For C_6H_5 and C_6D_5 (Table 2) experimentally determined polarizations are listed as *x*, *y*, and *z*. Experimental intensities are calculated according to eq 13, using CO_2 as internal standard. For p-C_6H_4D, p-C_6HD_4, o-C_6H_4D, and m-C_6H_4D (Tables 3 and 4), experimental intensities are listed as percentages of the base peak.

In the right columns of Tables 2–7 are listed calculated harmonic vibrational frequencies {ω} and intensities {A} from *ab initio* electronic structure calculations using the Gaussian 98 suite of programs.[68] We have chosen the hybrid-density functional theory (DFT) method with the exchange functional

(68) Frisch, M. J.; Trucks, G. W.; Schlegel, H. B.; Scuseria, G. E.; Robb, M. A.; Cheeseman, J. R.; Zakrzewski, V. G.; Montgomery, J. A., Jr.; Stratmann, R. E.; Burant, J. C.; Dapprich, S.; Millam, J. M.; Daniels, A. D.; Kudin, K. N.; Strain, M. C.; Farkas, O.; Tomasi, J.; Barone, V.; Cossi, M.; Cammi, R.; Mennucci, B.; Pomelli, C.; Adamo, C.; Clifford, S.; Ochterski, J.; Petersson, G. A.; Ayala, P. Y.; Cui, Q.; Morokuma, K.; Malick, D. K.; Rabuck, A. D.; Raghavachari, K.; Foresman, J. B.; Cioslowski, J.; Ortiz, J. V.; Stefanov, B. B.; Liu, G.; Liashenko, A.; Piskorz, P.; Komaromi, I.; Gomperts, R.; Martin, R. L.; Fox, D. J.; Keith, T.; Al-Laham, M. A.; Peng, C. Y.; Nanayakkara, A.; Gonzalez, C.; Challacombe, M.; Gill, P. M. W.; Johnson, B. G.; Chen, W.; Wong, M. W.; Andres, J. L.; Head-Gordon, M.; Replogle, E. S.; Pople, J. A. *Gaussian 98*, revision A.7; Gaussian, Inc.: Pittsburgh, PA, 1998.
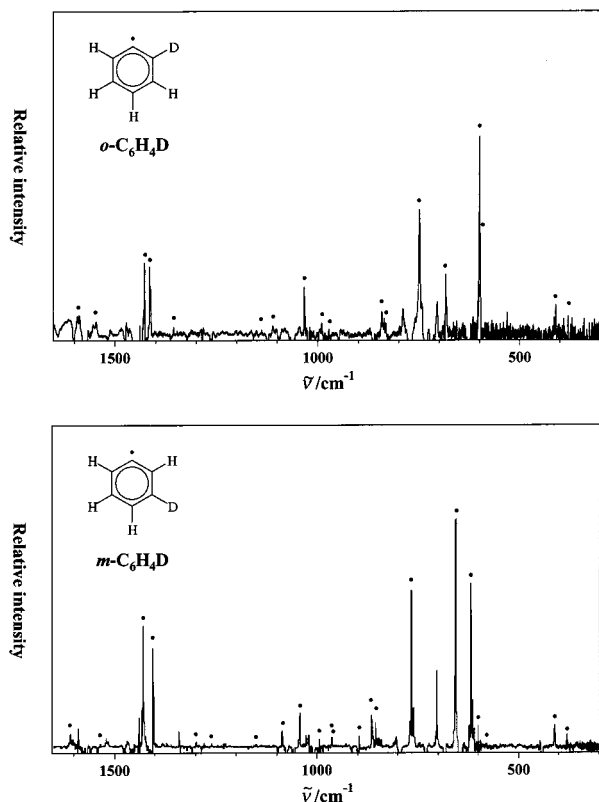
IR Spectrum of the Matrix-Isolated Phenyl Radical

J. Am. Chem. Soc., Vol. 123, No. 9, 2001 1983

Figure 5. Infrared spectra of o-C_6H_4D (top) and m-C_6H_4D (bottom). The spectra were obtained from matrix-isolated and -photolyzed, deuterated phenyl iodides. Peaks assigned to fundamentals are annotated (●). See also Tables 6 and 7.
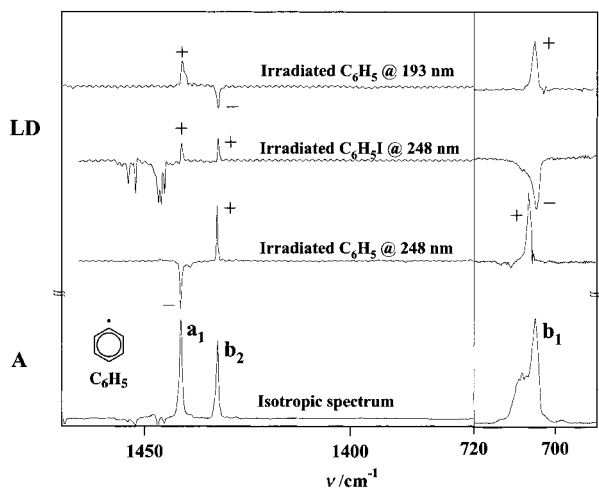

Figure 6. Linear dichroism of ν_{16} (706 cm^{-1}, b$_1$) ν_{22} (1432 cm^{-1}, b$_2$), and ν_5 (1441 cm^{-1}, a$_1$) in C_6H_5 after photoorientation by destruction of the radical with either 193 or 248 nm polarized light, and the linear dichroism of the same modes after photoorientation of C_6H_5 by photolysis of C_6H_5I with 248 nm polarized light.

of Becke,[69] UB3LYP, in combination with the cc-pVDZ or cc-pVTZ basis sets, which has proven to be very useful for modeling vibrational spectra of open shell hydrocarbons. Table 8 lists the calculated molecular properties of phenyl radical. The C–H bond lengths of benzene for all methods are all within 0.01 Å of the experimental value (1.084 Å), with the Hartree–Fock methods giving the poorest results. Density functional calculations appear to give fairly good results, especially with

(69) Becke, A. D. *J. Chem. Phys.* **1993**, *98*, 5648.

Table 2. Experimental Infrared Absorption Frequencies ($\tilde{\nu}$), Polarizations, and Absolute Intensities for the Phenyl Radical, C_6H_5, $\tilde{X}$) $^2A_1{}^a$

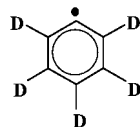|		experimental			calculated	
ν		$\tilde{\nu}$/cm^{-1}	pol.	A/km mol^{-1}	ω/cm^{-1}	A/km mol^{-1}
1	a$_1$	3086	z	3.1	3196	10.3
2		3072	z	0.2	3182	5.3
3		3037	z	0.2	3162	1.1
4		1581	z	2.2	1584	0.6
5		1441	z	8.7	1465	6.6
6		1154	–	0.1	1164	0.1
7		1027	z	7.9	1048	8.6
8		997	–	0.2	1022	0.3
9		976	z	1.6	981	1.6
10		605	–	1.4	614	1.8
11	a$_2$				967	0.0
12					815	0.0
13					401	0.0
14	b$_1$	972	–	0.1	999	0.2
15		874	–	0.9	894	0.3
16		706	x	55.9	721	52.6
17		657	x	1.1	673	13.6
18		416	x	3.4	426	5.1
19	b$_2$	3071	y	10.6	3184	21.6
20		3060	y	0.1	3169	4.1
21		1624	–	0.1	1639	1.9
22		1432	y	6.3	1457	5.3
23		1321	–	0.3	1340	0.4
24		1283	y	3.6	1293	0.1
25		1159	y	0.1	1165	0.2
26		1063	y	1.1	1070	3.8
27		587	–	0.2	597	0.6

^{a} The [unscaled] harmonic frequencies (ω) result from an *ab initio* electronic structure calculation, UB3LYP/cc-pVDZ. We estimate that the experimental frequencies are within 1% error of gas-phase values. Experimental intensities are determined using CO_2 as internal standard and has an uncertainty of about 15% (see text). The experimental polarizations (pol.) result from linear dichroism studies.

a larger basis set. The C–C bond lengths appear to adequate with all methods (1.397 Å in benzene) with the exception of the MP2 calculations. Only the density functional methods provided adequate spin expectation values, $\langle S^2 \rangle = 0.75$.

The vibrational frequencies were compared for the methods described above. The DFT harmonic frequencies $\{\omega\}$ produced the best match to experimentally measured frequencies $\{\tilde{\nu}\}$ with an average error of 2.0% for the cc-pVDZ basis set and 2.4% for the cc-pVTZ set. The errors for the HF/6-31G*, HF/6-311++G**, and MP2/6-31G** were 6.9, 6.0, and 9.3, respectively. Interestingly, the DFT method had significantly larger errors for the C–H stretching frequencies. This may be due to the relatively larger anharmonicity for these vibrational modes. The DFT methods also produced better matches of the infrared intensities (average error of about ±2 km mol^{-1} compared to ±5 km mol^{-1} for the other methods).

We have animated[70] the normal modes from a B3LYP/cc-pVDZ electronic structure calculation of the harmonic vibrational spectrum. Using our assignment (Table 2), this allows for a qualitative mapping of each absorption band to specific molecular vibrations. (Please see http://ellison.colorado.edu/

(70) *AnimateMode*, v. 2.0; Winter, P. R., Boulder, 1998, (computer program, part of Ph.D. Thesis, Department Chem., & Biochem., University of Colorado at Boulder).

Table 3. Experimental Infrared Absorption Frequencies ($\tilde{\nu}$), Polarizations, and Absolute Intensities for the 2,3,4,5,6-d_5 Phenyl Radical, C_6D_5, $\tilde{X}$ $^2A_1{}^a$

		experimental			calculated	
ν		$\tilde{\nu}$/cm^{-1}	pol.	A/km mol^{-1}	ω/cm^{-1}	A/km mol^{-1}
1	a_1	2292	z	0.2	2370	5.2
2		2290	z	0.4	2352	3.3
3		2282	z	0.7	2329	0.5
4		1494	z	0.1	1546	1.5
5		1314	z	1.3	1339	0.5
6		851	−	0.2	853	0.1
7		803	z	3.4	808	7.1
8		−	−	−	984	0.6
9		−	−	−	952	0.4
10		590	−	0.9	590	1.8
11	a_2				790	0.0
12					634	0.0
13					348	0.0
14	b_1	−	−	−	828	0.0
15		−	−	−	722	0.1
16		−	−	−	600	1.6
17		517	−	−	529	29.3
18		382	−	−	381	7.2
19	b_2	2271	y	1.0	2358	13.5
20		2264	y	0.5	2336	1.3
21		1561	y	0.1	1611	1.1
22		1312	y	0.5	1361	0.7
23		1297	y	0.8	1295	0.7
24		−	−	−	1011	0.2
25		−	−	−	844	0.3
26		806	y	1.9	807	2.9
27		547	−	−	572	0.7

^{a} The [unscaled] harmonic frequencies (ω) result from an *ab initio* electronic structure calculation, UB3LYP/cc-pVDZ. We estimate that the experimental frequencies are within 1% error of gas-phase values. Experimental Intensities are determined using CO_2 as internal standard and has an uncertainty of about 15% (see text). The experimental polarizations (pol.) result from linear dichroism studies.
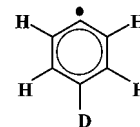
phenyl.) It can be shown,[71] that the normal modes of C_6H_5 (N_{VIB} = 27) can be directly correlated to those of benzene, C_6H_6 (N_{VIB} = 30), and that the three "missing" modes involves strong oscillations of the missing hydrogen in C_6H_5 along the molecular x, y, and z axis, respectively.

Individual Peak Assignments. The phenyl radical is known from EPR studies[19] to possess C_{2v} symmetry. The symmetries of the vibrational modes for C_6H_5, C_6D_5, p-C_6H_4D, p-C_6HD_4 are: $\Gamma_{vib}(C_{2v})$= 10 a_1 $\oplus$ 3 a_2 $\oplus$ 5 b_1 $\oplus$ 9 b_2. The *ortho* and *meta* deuterated radicals only have C_s symmetry so that both o-C_6H_4D and m-C_6H_4D possess $\Gamma_{vib}(C_s)$ = 19 a' $\oplus$ 8 a'' modes.

The individual peak assignments are justified in the following list of observed spectral features. All of the 24 IR-active modes of C_6H_5 were observed by use of our recently developed method (flash pyrolysis and supersonic expansion), Figure 3.

416 cm^{-1} (ν_{18}) b$_1$. The lowest-frequency transition that we measured was located at 416 cm^{-1} (ν_{18}). When measured on a matrix of irradiated C_6H_5I, the observed transition frequency shifts to 414 cm^{-1}, which might be due to perturbation from iodine atom. For the C_{2v} deuterated isotopomers the shifts of this peak are consistent with the calculated shifts.

(71) Friderichsen, A. V.; Nimlos, M. R.; Winter, P. R.; Ellison, G. B. In progress.

Table 4. Experimental Infrared Absorption Frequencies ($\tilde{\nu}$) and Relative Intensities (Expressed as Fraction of Base Peak) for the 4-d Phenyl Radical, p-C_6H_4D, $\tilde{X}$) $^2A_1{}^a$

		experimental		calculated	
ν		$\tilde{\nu}$/cm^{-1}	A/%	ω/cm^{-1}	A/km mol^{-1}
1	a_1	−	−	3186	0.1
2		−	−	3167	7.1
3		−	−	2356	4.9
4		−	−	1575	0.9
5		1435	21	1462	6.3
6		1155	1	1164	0.1
7		1031	15	1047	8.3
8		−	−	1012	0.1
9		962	8	971	2.2
10		599	3	608	1.7
11	a_2			967	0.0
12				815	0.0
13				401	0.0
14	b_1	931	2	961	0.2
15		808	54	825	17.5
16		681	26	698	9.3
17		587	100	600	35.5
18		400	7	410	2.5
19	b_2	−	−	3184	21.6
20		−	−	3169	4.1
21		1602	2	1633	1.2
22		1372	19	1402	4.1
23		−	−	1339	0.6
24		−	−	1288	0.0
25		1084	5	1096	2.9
26		863	5	867	1.0
27		−	−	593	0.6

^{a} The [unscaled] harmonic frequencies (ω) result from an *ab initio* electronic structure calculation, UB3LYP/cc-pvdz. We estimate that the experimental frequencies are within 1% error of gas-phase values.

587 cm^{-1} (ν_{27}) b$_2$. We only observed this transition using photolyzed or flash pyrolyzed iodobenzene, eq 5 or 8. The observed peak shifts in the spectra of C_6D_5 match the calculated values. This peak was not observed for the other C_{2v} isotopomers.
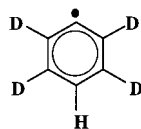
605 cm^{-1} (ν_{10}) a$_1$. We observed this transition using eqs 2, 3, 5, or 8. The observed shifts for this peak in the spectra of the deuterated isotopomers matched the calculated values. The peak in the p-C_6HD_4 spectrum is a combination of this transition and ν_{16} as indicated by the width of the peak.

657 cm^{-1} (ν_{17}) b$_1$. An intense IR peak is located at 657 cm^{-1} and is a C−H bending mode that corresponds to the intense 674 cm^{-1} (a_{2u}) band of benzene.[72,73] This peak was observed using eqs 2, 6, or 8. In photolysis experiments with benzoyl peroxide the carbon dioxide transition obscured this transition, but during pyrolysis experiments it could be resolved. As with ν_{16}, the frequency of this transitions is perturbed slightly by iodine atom in the photolysis of C_6H_5I (1 cm^{-1} red shift). The observed shifts for the isotopomers are consistent with calculations.

706 cm^{-1} (ν_{16}) b$_1$. The most intense feature in the IR spectrum of C_6H_5 occurs at 706 cm^{-1}. This is the C−H bending mode similar to the mode in C_6H_6 at 682.5 cm^{-1}, which is also the most intense vibrational transition. We have positively

(72) Brown, K. G.; Person, W. B. *Spectrochim. Acta A* **1978**, *34A*, 117.
(73) Dang-Nhu, M.; Pliva, J. *J. Mol. Spectrosc.* **1989**, *138*, 423.

Table 5. Experimental Infrared Absorption Frequencies ($\tilde{\nu}$) and Relative Intensities (Expressed as Fraction of Base Peak) for the 2,3,5,6-d_4 Phenyl Radical, p-C_6HD_4, $\tilde{X}\ ^2A_1{}^a$

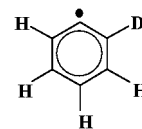|		experimental		calculated	
ν		$\tilde{\nu}/cm^{-1}$	$A/\%$	ω/cm^{-1}	$A/km\ mol^{-1}$
1	a_1	−	−	3186	9.9
2		−	−	2360	0.1
3		−	−	2336	3.8
4		1529	3	1553	1.2
5		1329	−	1346	0.6
6		966	−	853	0.1
7		950	−	811	6.9
8		852	1	993	0.4
9		807	23	958	0.6
10		587	27	595	1.9
11	a_2			790	0.0
12				634	0.0
13				348	0.0
14	b_1	913	20	936	4.9
15		756	2	775	0.8
16		587	3	582	27.5
17		568	100	600	1.7
18		380	18	389	10.2
19	b_2	−	−	2358	13.7
20		−	−	2336	1.3
21		1570	3	1618	1.8
22		1395	13	1416	2.5
23		1309	10	1319	0.4
24		−	−	968	0.0
25		1127	1	1141	0.4
26		801	5	808	2.7
27		−	−	576	0.6

^{a} The [unscaled] harmonic frequencies (ω) result from an *ab initio* electronic structure calculation, UB3LYP/cc-pVDZ. We estimate that the experimental frequencies are within 1% error of gas-phase values.

Table 6. Experimental Infrared Absorption Frequencies ($\tilde{\nu}$) and Relative Intensities (Expressed as Fraction of Base Peak) for the 2-d Phenyl Radical, o-C_6H_4D, $\tilde{X}\ ^2A_1$

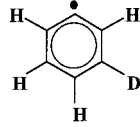|		experimental		calculated	
ν		$\tilde{\nu}/cm^{-1}$	$A/\%$	ω/cm^{-1}	$A/km\ mol^{-1}$
1	a'	−	−	3195	12.6
2		−	−	3183	15.2
3		−	−	3172	9.7
4		−	−	3164	0.6
5		−	−	2349	2.3
6		1587	−	1634	2.0
7		1547	−	1581	0.5
8		1429	17	1453	5.1
9		1413	33	1441	4.6
10		1356	−	1340	0.4
11		−	−	1248	0.1
12		1139	−	1164	0.2
13		1111	−	1125	1.1
14		1034	17	1052	6.4
15		991	1	1015	0.6
16		−	−	978	0.6
17		832	2	842	3.9
18		598	−	609	2.1
19		−	−	591	0.6
20	a''	973	2	996	0.0
21		−	−	952	0.5
22		842	8	866	0.6
23		748	100	762	26.0
24		685	13	699	7.4
25		601	75	613	22.6
26		401	−	421	5.3
27		378	−	381	1.4

^{a} The [unscaled] harmonic frequencies (ω) result from an *ab initio* electronic structure calculation, UB3LYP/cc-pvdz. We estimate that the experimental frequencies are within 1% error of gas-phase values.
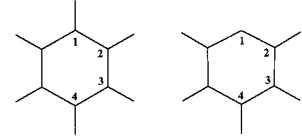
identified this transition because the same peak is seen in the spectra recorded using eq 2−8. The transition in C_6H_5 produced from the photolysis of C_6H_5I shows a 2 cm^{-1} shift due to the interaction of iodine with the hydrogen atoms. Our assignment is confirmed by DFT electronic structure calculations and polarization experiments. The transition exhibits positive dichroism when C_6H_5 is destroyed with 248 nm polarized light (A_1 electronic transition) and a positive dichroism when destroyed with polarized 193 nm light (B_2 electronic transition). This indicates that the vibrational transition has b_1 symmetry (see Figure 6). The observed peaks in the isotopomer spectra have shifts consistent with the calculated shifts.

874 cm^{-1} (ν_{15}) b_1. This feature was observed using eqs 2, 3, 5, or 8. The band was too weak to clarify the sign of dichroism. However, the observed spectral shifts agree with calculations and we assign this peak to the ν_{15} mode in the b_1 symmetry block.

972 cm^{-1} (ν_{14}) b_1. This band appears as a very weak feature in the spectrum when using eqs 2, 3, or 8. The peak in the spectrum of photolyzed C_6H_5I is shifted by 1 cm^{-1}. A positive dichroism was observed after photolysis of C_6H_5 with polarized 193 and 248 nm light. The observed isotopic shifts for p-C_6H_4D and p-C_6HD_4 agree with calculated values.

976 cm^{-1} (ν_9) a_1. This peak was observed in spectra collected using eqs 2, 3, 5, or 8, though the peak from photolyzed C_6H_5I had shifted by (3−4 cm^{-1}) and split into a doublet. The peak

showed a negative dichroism when exciting C_6H_5 (created using iodobenzene or benzoyl peroxide) with 248 nm light indicating that the transition has a_1 symmetry. The doublet is also observed in the isotopomers prepared from photolyzed iodobenzenes and all of the observed shifts agree with calculations.

997 cm^{-1} (ν_8) a_1. This was a very weak peak observed when using eqs 2, 3, 5, or 8. Using eq 5 or 8, the band was obscured by a strong precursor band at 999 cm^{-1} (thus, the apparent high intensity in Figure 3). The observed spectral shifts for the deuterated isotopomers agree with calculations.

1027 cm^{-1} (ν_7) a_1. This was a strong peak found in the spectrum using eqs 2, 3, 5, or 8. In the spectrum from photolyzed C_6H_5I there are two peaks, at 1028 cm^{-1} and 1025 cm^{-1}, respectively. The peak shows a negative dichroism upon photolysis of C_6H_5 with polarized 248 nm light and a positive dichroism upon photolysis with polarized 193 nm light indicating that the symmetry of the vibration is a_1. For the isotopomers the shifts are consistent with the calculations. With the iodo compounds the doublet is maintained in the isotopomers.

1063 cm^{-1} (ν_{26}) b_2. This feature is a band of medium intensity. As in the case of ν_8, the band is obscured by a strong precursor peak in the matrix made from photolyzed or flash pyrolyzed C_6H_5I. We determined the symmetry of this vibration by destroying C_6H_5 with polarized 193 or 248 nm light and measuring the linear dichroism. The observed isotopomer shifts agree well with calculations. Polarization data for the d_5 isotopomer also helped with the assignment (Table 3). The

Table 7. Experimental Infrared Absorption Frequencies ($\tilde{\nu}$) and Relative Intensities (Expressed as Fraction of Base Peak) for the 3-d Phenyl Radical, m-C$_6$H$_4$D, $\tilde{X}$ ^{2}A$_1$[a]

ν		experimental $\tilde{\nu}$/cm^{-1}	A/%	calculated ω/cm^{-1}	A/km mol^{-1}
1	a′	—	—	3192	12.8
2		—	—	3182	8.4
3		—	—	3180	5.9
4		—	—	3165	3.4
5		—	—	2346	7.1
6		1609	6	1634	1.8
7		1535	1	1573	1.4
8		1430	42	1455	5.9
9		1404	26	1432	3.5
10		1299	1	1330	0.5
11		1261	1	1274	0.1
12		1150	—	1164	0.1
13		1086	7	1093	3.1
14		1044	12	1057	6.8
15		994	1	1017	0.2
16		962	1	974	0.7
17		855	7	859	3.4
18		601	2	610	1.6
19		578	—	591	0.6
20	a″	965	2	987	0.5
21		896	—	917	1.7
22		863	14	884	3.2
23		767	49	783	14.5
24		657	100	675	26.0
25		617	64	631	14.4
26		410	7	421	5.2
27		380	—	383	0.9

[a] The [unscaled] harmonic frequencies (ω) result from an *ab initio* electronic structure calculation, UB3LYP/cc-pvdz. We estimate that the experimental frequencies are within 1% error of gas-phase values.

intensities and symmetries of ν_7 and ν_{26} correlate well with the 1038 cm^{-1} transition in C$_6$H$_6$, which is a doubly degenerate e$_{1u}$ vibration. As the symmetry in C$_6$H$_6$ is broken from D_{6h} to C_{2v} the e$_{1u}$ modes decompose to a$_1$ ⊕ b$_2$.

1154 cm^{-1} (ν_6) a$_1$. This weak feature occurs in spectra obtained from nitrosobenzene, benzoyl peroxide and iodobenzene. The peak is red-shifted to 1151 cm^{-1} in the spectra obtained from photolyzed iodobenzene. Observed isotopic shifts are consistent with calculations.

1159 cm^{-1} (ν_{25}) b$_2$. This weak peak occurs in spectra using eqs 2, 3, 5, or 8. It shows a positive dichroism upon photolysis with 248 nm light which is consistent with the assignment of b$_2$ symmetry. The isotopomeric shifts are consistent with calculations.

1283 cm^{-1} (ν_{24}) b$_2$. This is a weak feature and found using eqs 2, 3, 5, or 8, though there is a 2 cm^{-1} shift when made from photodissociated C$_6$H$_5$I. It shows a positive dichroism upon photolysis with polarized 248 nm light. In the isotopomer spectra, the peak was only observed in the spectrum of C$_6$D$_5$. Polarization results for C$_6$D$_5$ were consistent with our symmetry assignments.

1321 cm^{-1} (ν_{23}) b$_2$. This weak band is observed in the spectra from photolyzed benzoyl peroxide, eq 3, but is obscured by the precursor when using eq 2 or 5. In flash-pyrolyzed C$_6$H$_5$I, eq 8, we observe the peak as a shoulder (to the red) on the C$_6$H$_5$I band centered at 1321.3 cm^{-1}. It shows a positive

Table 8. *Ab Initio* Electronic Structure Calculations Were Used To Find the Molecular Properties of C$_6$H$_5$ and To Compare between Different Methods[a]

	HF/ 6-31++G**	MP2/ 6-31G**	UB3LYP/ cc-pVDZ	UB3LYP/ cc-pVTZ
r(C−H$_2$)	1.075	1.081	1.093	1.082
r(C−H$_3$)	1.076	1.083	1.093	1.083
r(C−H$_4$)	1.075	1.081	1.092	1.082
r(C$_1$−C$_2$)	1.386	1.356	1.381	1.371
r(C$_2$−C$_3$)	1.402	1.374	1.407	1.399
r(C$_3$−C$_4$)	1.400	1.372	1.399	1.392
$\langle S(S+1) \rangle$	1.120	1.145	0.750	0.750

[a] Bond lengths are reported in Å while $\langle S(S+1) \rangle$ is the spin expectation value. An experimental geometry for the C$_6$H$_5$ radical has not been reported. A doublet species such as phenyl, $\tilde{X}$ ^{2}A$_1$, must have $\langle S^2 \rangle = {}^3/_4$. For comparison the experimental bond[78] lengths in C$_6$H$_6$ are r(C−H) = 1.084 Å and r(C−C) = 1.397 Å.

dichroism upon photolysis with polarized 248 nm, consistent with our assignment of b$_2$ symmetry.

1432 cm^{-1} (ν_{22}) b$_2$ and 1441 cm^{-1} (ν_5) a$_1$. The second most intense vibrational transitions are the doublet located at 1441 cm^{-1} (ν_5) and 1432 cm^{-1} (ν_{22}). The vibrations giving rise to these transitions are carbon bond stretches and in-plane bends involving hydrogen atoms. The symmetries of these vibrations were determined with two different polarization experiments. When we destroy C$_6$H$_5$ with polarized 248 nm (A$_1$) light, we measure a positive dichroism for ν_{22} and a negative dichroism for ν_5. When irradiated with polarized 193 nm light (B$_2$) we measure a negative dichroism for ν_{22} and a positive dichroism for ν_5. This indicates that ν_{22} has b$_2$ symmetry, while ν_5 has a$_1$ symmetry (see Figure 6). These transitions correspond to the observed, doubly degenerate (e$_{1u}$), 1482 cm^{-1} transition in benzene.

1581 cm^{-1} (ν_4) a$_1$. This peak is observed in the spectra when using eq 2 or 3 but is obscured by a C$_6$H$_5$I band when we use eq 5 or 8. It has a negative dichroism upon photolysis with polarized 248 nm light which is consistent with our a$_1$ symmetry assignment. The isotopic shifts are consistent with calculations. Polarization spectra of C$_6$D$_5$ confirm our symmetry assignments.

1624 cm^{-1} (ν_{21}) b$_2$. This weak peak is observed in spectra using both eqs 2 and 3, but is obscured by a precursor band in C$_6$H$_5$I, as is ν_4.

C−H Stretching Region. We observe all five predicted C−H stretching vibrations, using eqs 2, 3, 5, or 8 (Figure 3, Table 2). In all cases, precursor as well as side-product bands obscured the spectrum and made the assignment difficult. Based on the bands that consistently were observed in all experiments, coupled with their sign of dichroism after photoorientation using 193 or 248 nm polarized light, we assign the following observed bands in this region to phenyl radical: 3037 cm^{-1} (ν_3, a$_1$), 3060 cm^{-1} (ν_{20}, b$_2$), 3071 cm^{-1} (ν_{19}, b$_2$), 3072 cm^{-1} (ν_2, a$_1$), and 3086 cm^{-1} (ν_1, a$_1$).

Gas-to-Matrix Shifts. The vibrational frequencies reported here are likely to be slightly shifted, compared to gas-phase

values. This is due to perturbations from the host Ar atoms surrounding the "isolated" radical. The perturbation might also affect the infrared absorption cross sections, and thus the band intensities.

Jacox has reviewed the matrix shifts for a large number of diatomic and small polyatomic free radicals and ions trapped in Ne and Ar matrices.[74,75] The overall conclusion that could be made for polyatomic free radicals in Ar matrices was that the shift is less than 1% and usually to the red. Benzyl radical, $C_6H_5CH_2$, a radical similar in structure and size to C_6H_5, might serve as good candidate for comparison. The average and standard deviation of the shifts for six modes in the range $350-1550$ cm^{-1} is $+0.7 \pm 0.2\%$, all bands being shifted to red. No values were reported for the C−H stretching region for C_6H_5-CH_2. However, the distribution of matrix shifts for the subset of hydrogen stretching vibrations in all the reviewed species has its maximum at $+0.3\%$, which is 9 cm^{-1} for a band centered at 3000 cm^{-1}.

One might also consider the matrix shift of benzene. We have prepared an Ar matrix of C_6H_6, measured the infrared spectrum, and compared it to the reported gas-phase benzene values summarized by Dang-Nhu and Pliva.[73] The shifts of the three strong bands, ν_4 (673 cm^{-1}, a_{2u}), ν_{13} (1483 cm^{-1}), and ν_{14} (1038 cm^{-1}), are -1.3, $+0.6$, and -2.5 cm^{-1}, respectively, an average of $-0.13 \pm 0.15\%$. In the C−H stretching region, three overlapping bands of comparable strengths have been observed and can be interpreted as a Fermi/Coriolis resonance triad of ν_{12} (3047.908 cm^{-1}, e_{1u}) with $\nu_{13} + \nu_{16}$ (1483.985, $e_{1u} +$ 1609.518, e_{2g}) and $\nu_2 + \nu_{13} + \nu_{18}$ (993.063, $a_{1g} + 1483.985$, $e_{1u} + 608.13$, e_{2g}).[76,77] In our Ar matrix, this Fermi resonance splitting is enhanced and the three bands resolved and centered at 3048, 3080, and 3100 cm^{-1}, respectively, which is in good agreement with the matrix frequencies reported by Brown and Person.[72] Although none of the overtones or combination bands of the strongest fundamentals in the a_1 block (ν_5 and ν_7) and the b_2 block (ν_{22} and ν_{24}) of C_6H_5 fall within the $3000-3100$ cm^{-1} range, Fermi resonance bands cannot be excluded.

On the basis of these considerations, the matrix shifts for C_6H_5 can be expected to be less than 1% for all vibrational frequencies, including C−H stretches. Considering ν_4, ν_{13}, and ν_{14} in C_6H_6, it is not clear whether the shifts will be to the red or to the blue. However, it seems from the review by Jacox[75] that neutral hydrocarbon radicals in general have positive (to the red) matrix shifts. Gunion et al.[24] produced the phenyl radical by photodetachment, $C_6H_5^- + \hbar\omega_{351\ nm} \rightarrow C_6H_5 + e^-$. They reported two gas-phase a_1 fundamentals of C_6H_5. The first, $\tilde{\nu}_a = 600 \pm 10$ cm^{-1}, was assigned as ν_{10} and is in agreement with our observed ring breathing mode, ν_{10}, at 605 ± 1 cm^{-1}. A second feature was observed in the photodetachment study at $\tilde{\nu}_b = 968 \pm 15$ cm^{-1}. Identification of ν_b was uncertain but in the light of our present results this fundamental seems to be identical to ν_9, (also a ring-breathing mode) observed in the Ar matrix at 976 ± 1 cm^{-1}.

Uncertainties of IR Frequencies and Intensities. The line widths (fwhm) of the IR bands in our matrix spectra are $0.5-0.8$ cm^{-1}, and a conservative estimate of the error of the reported frequency values due to matrix inhomogeneous line broadening is ±0.4 cm^{-1}. We thus estimate the total error (line broadening

and matrix shift), in the terms of deviation from the true gas-phase values, for the frequencies in Tables $2-7$ as:

$$\tilde{\nu}_{gas} = (\tilde{\nu}_{matrix} \pm 0.4\ cm^{-1}) \pm 1\% \approx \tilde{\nu}_{matrix} \pm 1\% \quad (14)$$

For the errors on the absolute intensities in the IR spectra of C_6H_5 and C_6D_5, calculated using CO_2 as internal standard, we need to evaluate:

$$s_{A(C_6H_5)} =$$

$$A(C_6H_5)\sqrt{\left(\frac{s_{A(CO_2)}}{A(CO_2)}\right)^2 + \left(\frac{{}^s\int_{C_6H_5}d\tilde{\nu}[OD]}{\int_{C_6H_5}d\tilde{\nu}[OD]}\right)^2 + \left(\frac{{}^s\int_{CO_2}d\tilde{\nu}[OD]}{\int_{CO_2}d\tilde{\nu}[OD]}\right)^2}$$
$$(15)$$

where s is the standard deviation. We have used the software package Omnic 5.0, Nicolet Instruments, to calculate the integrated band intensities, and find a standard deviation of $5-12\%$, depending on the signal-to noise ratio and band shape, using this technique. The error is due to the subjective choice of baseline and of integration limits. The relative error of $A(CO_2)$, as reported by Radziszewski et al.,[62] is 3% for both ν_2 (661 cm^{-1}, 62 ± 2 km mol^{-1}) and ν_3 (2348 cm^{-1}, 485 ± 15 km mol^{-1}). Evaluation of the square root in eq 15, using 3% for the first term, and 10% for the second and third, gives a relative standard deviation, s_A/A, of 15%. We estimate that the uncertainty for the infrared bands is roughly 15%.

IV. Conclusions

The infrared vibrational absorption spectrum of phenyl radical and five deuterated isotopomers have been established. As a result of this more thorough study, the C_6H_5 frequencies from this paper supersede our earlier values reported in *J. Am. Chem. Soc.* **1996**, *118*, 7400−7401. Three different methods have been used for independent production of phenyl radical in an Ar matrix: photodissociation of matrix isolated precursors, vacuum pyrolysis in an effusive thermal source, and flash pyrolysis in a hyperthermal nozzle. Several different precursors have been applied, as well as the use of isotopically labeled precursors, to establish a firm assignment. Photoorientation followed by linear dichroism spectroscopy provided a powerful criteria in the assignments of vibrational bands in terms of their polarization. The use of benzoyl peroxides and nitrosobenzenes provided CO_2 and NO as internal standards for determination of experimental intensities. Experimental frequencies of C_6H_5 and deuterated isotopomers were in good agreement with DFT modeled harmonic frequencies. Taking the gas-to-matrix shifts into account, as well as matrix inhomogeneous line broadening, the vibrational frequencies reported are within ±1% error of unperturbed gas-phase values.

(74) Jacox, M. E. *J. Mol. Spectrosc.* **1985**, *113*, 286−301.
(75) Jacox, M. E. *Chem. Phys.* **1994**, *189*, 149−170.
(76) Brodersen, S.; Langseth, A. *Mat. Fys. Skr., Kgl. Dan. Vid. Selsk.* **1956**, *1*, 1−45.
(77) Pliva, J.; Pine, A. S. *J. Mol. Spectrosc.* **1982**, *93*, 209−236.
(78) Herzberg, G. H. *Molecular Spectra and Molecular Structure: Electronic Spectra and Electronic Structure of Polyatomic Molecules*; D. Van Nostrand: Princeton, New Jersey, 1967; Vol. III.

JA0024338